Numerical modelling of ODS steel tube cold pilgered by HPTR. Focus on experimental measurements and simulation of residual stress.

D. Sornin, E. Pachon, E. Vanegas-Marques, R. Loge, K. Mocellin

Numerical modelling of ODS steel tube cold pilgered by HPTR. Focus on experimental measurements and simulation of residual stress.

D. Sornin [*1] , E.A. Pachon[1a] , E. Vanegaz-Marquez[2b], R. Logé[2c] , K. Mocellin[2]

[1] CEA, DEN, Service de Recherches Métallurgiques Appliquées, 91191 Gif-sur-Yvette, France.
[2] Mines-ParisTech, CEMEF - Centre de Mise en Forme des Matériaux, CNRS UMR 7635, 06904 Sophia Antipolis cedex, France.
[a] Actual adresse : ArcelorMittal Maizières Research SA, Voie Romaine, 57283 Maizières-les-Metz, France.
[b] Actual adresse : Lisi Aerospace, 18 rue Jean Vaurs, 12200 Villefranche-de-Rouergue, France.
[c] Actual adresse : Thermomechanical Metallurgy Laboratory – PX Group Chair, Ecole Polytechnique Fédérale de Lausanne (EPFL), CH-2002 Neuchâtel, Switzerland.
[*] Corresponding author: denis.sornin@cea.fr

Abstract. Oxides Dispersed strengthened (ODS) stainless steels are foreseen for fuel cladding tubes in the coming generation of fission sodium cooled nuclear reactors. Classically those steels are cold formed as cladding tubes by a sequence of milling passes with intermediate heat treatments. This study focuses on numerical simulation of tube cold pilgering by High Precision Tube Rolling (HPTR). A 3D Finite Element Method mechanical analysis of the HPTR process is proposed. Results are confronted to experiments regarding geometry and residual stress.
Key words: Cold Pilgering, ODS stainless steel, 3D finite element method, tube forming, residual stress

1 Introduction

Oxide Dispersion Strengthened (ODS) ferritic/martensitic steels provide the needed mechanical strength and show favourable properties for high temperature and high burn-up applications in the coming generation of fission nuclear reactors (SFR). Indeed, the high density of finely dispersed oxide particles of nanometric scale, that act as obstacles upon moving dislocations, improve the high temperature strength of ODS materials. Many works are driven to develop ODS materials for nuclear applications; (e.g. [1],[2]) and specific studies were conducted to propose ODS steels as fuel cladding tube [3],[4]. Classically, the cladding tubes are cold formed by a sequence of cold pilger rolling passes with intermediate heat treatments to reduce the strain hardening induced by the cold work. Residual stress (RS) appears as a crucial issue regarding service duty and forming operation design. For this study the HPTR (High Precision Tube Rolling) technology is used to produce ODS steel tubes. RS field ensue from a complexes load path prospected by FEM simulations. Therefore, experimental and numerical results are compared and highlight the need of a more accurate modelling of tube pilgering technology

2 Tube processing

HPTR cold pilgering process is a cyclic tube forming operation where the material is repeatedly deformed over a fixed cylindrical mandrel by three grooved dies rolling along the tube. The axisymmetric dies rotate around their axis (see fig. 3) and roll without sliding along the tube wall, following the kinematic given by cams [5] (see fig. 1). During pilgering operation the inner radius and wall thickness are both progressively reduced. Once the external diameter is reached, a hillock warrants the tube calibration without any slope (position 3 Figure 1). In the same time the internal surface is calibrated by the axisymmetric mandrel. A pinion-rack gearing system, after each back and forth movement (stroke) of the dies (position 1 Figure 1), moves ahead (few mm) and rotates (between 30° and 90°) the tube around its axis. It is important that the rotation angle is not multiple of π as to avoid tube polygonalization.

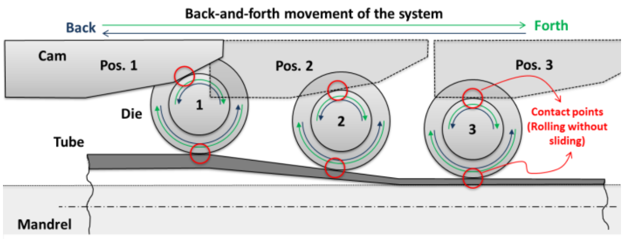

Figure 1: Schematic representation of the back and forth movement of the HPTR pilgering mill.

On the CEA HPTR facilities an ODS steel (Fe-14Cr-1W-0.3Ti-0.25Y_2O_3) tube is submitted to a pilgering sequence. The mother tube is 15.97 mm in diameter and 1mm thick whereas the finished tube is 14.38 mm in diameter and 0.8 mm thick.

[a] Corresponding author: denis.sornin@cea.fr

The transition region (i.e. from the last rough to the first finished section) is about 200mm. The grooved dies diameter is 45 mm in the deep of the groove. The section of the groove corresponds to the section of the finished tube. The tube is moved forward (feed) 1,7mm and rotated (39°) after each stroke.

3 Experiments

After forming, the transition region is sliced into 36 rings of 5 mm. Each ring, numbered from the finished (n°1) to the mother (n°36), is submitted to geometrical measurements as to determine the inner and outer diameter. Two hardness (HV1) indentations are performed on the cross section and distance between the two points measured (Figure 2 .a).

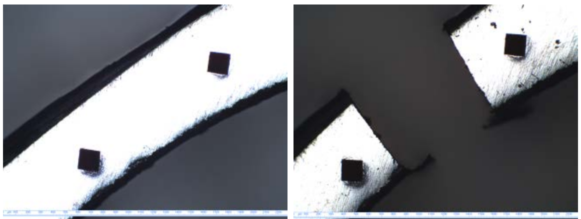

Figure 2: Hardness indentation, (a) before cutting, (b) after cutting and relaxation.

Then, the ring is mechanically sliced (0.5 mm thick saw) along the axis direction as to relax a part of tangential residual stresses (Figure 2.b). The distance between the two points is measured a second time as to determine Δd (μm) the relaxation distance.

As presented in Figure 3 tube samples are sliced by (Electric Discharge Machining (EDM).

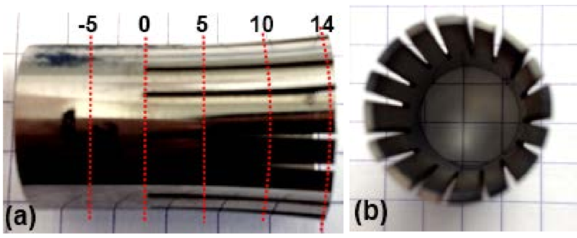

Figure 3: Calibrated tube after EDM machining, (a) side view showing blade bending, (b) axial view.

Residuals stress relaxation in the axial direction tends to bend the blades. This protocol is applied to the rough and calibrated tube section.

The part of residual stress relaxed by the both kind of samples is determined assuming a purely elastic relaxation and a Young modulus fixed at 205 GPa. Thickness is considered as negligible regarding diameter. For the ring samples the following equation is used assuming a linear dependence of stress through the thickness

$$\sigma_{\theta\theta}(\text{skin}) = \frac{\text{e.E.}\Delta\text{d}}{2\pi.\emptyset.\emptyset_0} \qquad \text{(Eq. 1)}$$

where e is the thickness, E the young modulus, Ø and $Ø_0$ the final and initial diameters respectively.

For blade relaxation laser metrology is performed on 5 sections. All the blades show approximately the same shape, then, the average of the 8 measures is used. Those data are fitted with a second order polynomial function

$$y(x) = \text{A}.x^2 + B.x \qquad \text{(Eq. 2)}$$

where, B correspond to the rigid motion of the blade and A is related to the relaxed axial stress σ_{zz} following the equation:

$$\sigma_{zz}(\text{skin}) = \text{e.E.A} \qquad \text{(Eq. 3)}$$

A is fitted at 6.5 10^{-3} N.

4 Numerical Set-up

Numerical modelling of HPTR has been recently addressed by *Vanegas & al* [6]. This study concludes to the need to use mixed kinematic and isotropic hardening as to traduce the cyclic loading involved by pilgering.

More recently CEA performed FEM simulations using the MSC-MARC® software.

To correctly capture gradients within the tube the refined region is discretized with 4 elements through the thickness. The forming sequence implies simulation of 123 back and forth strokes. To ensure an accurate contact description between the tools and the part the step time is fixed at 1000 time increment per stroke.

Plastic behaviour is described by an elastoplastic *Chaboche* like model implemented in MSC-MARC®.

The yield locus is classically defined as

$$f = J2\left(\underline{\sigma} - \underline{X}\right) - R - \sigma_y \qquad \text{(Eq. 4)}$$

Where $\underline{\sigma}$ is the stress tensor, $\underline{X}$ kinematic hardening, and R and σ_y the isotropic hardening and initial yield stress.

Kinematic and isotropic hardening are assumed non-linear and defined by the classic relations

$$X = \frac{2}{3}\underline{C}:\dot{\varepsilon}p - \alpha X\dot{p} \text{ and } R = Q(1 - b.exp^{-bp}) \quad \text{(Eq. 5)}$$

Where C, Q, α and b are material constants. Those parameters, listed in table 1, are identified to the ODS steels material using alternate compression tests described in [7].

Table 1. Behaviour law parameters identified to ODS steel.

	parameter	value	unit
Kinematic hardening	C	81092	MPa
	α	209	
Isotropic hardening	Q	340	MPa
	b	4	
Elastic constant	σ_y	960	MPa
	E	205	GPa
	ν	0.3	

Therefore, resulting of the non-linear behaviour law, a few thousand of elements and the 1.2 10^5 time step the simulation implies massive computational costs. As to jugulate this problem, only one third of the tube structure is studied and symmetry boundary conditions are applied to simulate reactions of the rest of the structure.

The complete numerical set-up as well as the major results will be discussed on a coming communication. Stress results presented above are extracted using numerical sensors placed on the outer skin of the tube in the middle of the refined region.

5 Results and discussion

Figure 5 presents the experimental and numerical evolutions of the tangential stress along the tube axis.

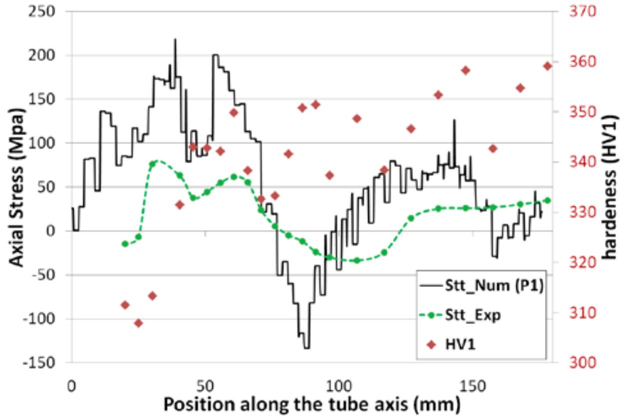

Figure 4: Experimental (dash) and computed (plain) tangential stress component along the tube axis. Hardness points are plotted with dots.

It appears that numerical results are approximately two times higher than experimental ones. The global shape of residual stress repartition along the tube is consistent between the two methods. Waves observed for the computed curve are due to numerical approximation mainly related to the contact algorithm. Moreover, hardness is also plotted and shows a brutal increase of hardness at the beginning of the process followed by a moderate and monotonic rise until 400HV. Hardness is not correlated to the RS evolution.

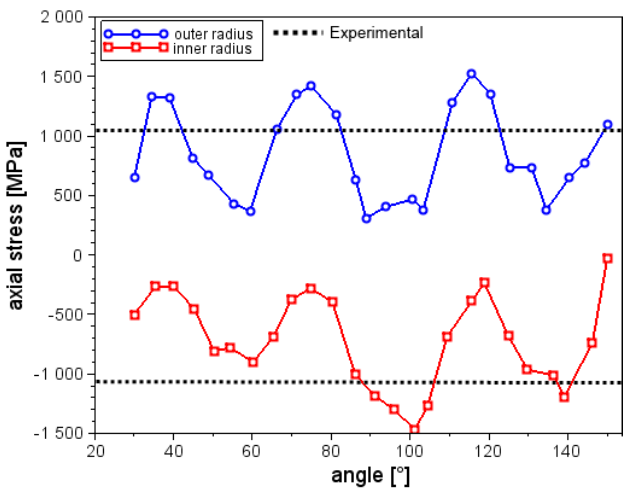

Figure 5: Axial stress evolution along circumference of the tube, computed (plain) and experimental (dash) values.

Measurement of the blade deformation on the sample extracted from the mother tube reveals no bending. It allow us to confirm that heat treatment between rolling sequence are efficient to release 1st order stress components. Figure 6 presents the evolution of the computed axial stress σ_{zz} at the outer an inner skin of the finished tube for various positions along the circumference (120°).

The maximum stress (inner and outer skin) are experimentally evaluated at 1066 MPa and also plotted in dash line. The external skin seems submitted to a strong tension stress (about Rp02 of the material) and numerical simulation seems to underestimate this value. Simulation exhibits there a curious stress field. The difference between the inner and outer skin stress values is approximately constant explaining the homogenous relaxation of blades (Figure 3.b) whereas the intensity and sign of the axial stress component evolves along the circumference. This particular behaviour could have a determinant impact on the tube behaviour during and after forming especially regarding damage and crack propagation. Therefore, we suggest to prospect residual stress field by X Ray Diffraction (XRD) on various position of the circumference to confirm this first observation.

6 Conclusions

ODS steel tubes are produced by the HPTR tube pilgering technology. Those tubes are submitted to ring and blades relaxation tests to determine the intensity of tangential and axial residual stress contribution. Those experimental data are exploited, assuming a purely elastic spring back, and compared to numerical results issued from FEM simulation of the process. From the numerical point of view, the very high number of increments needed to simulate this incremental process reveals the need of an improved accuracy and stability of the numerical schemes. This study reveals also a peculiar (oscillating) flied of axial stress along the circumference and a complex path of tangential stress. Therefore, we plane to prospect residual stress field by XRD in order to assess those first results.

Acknowledgements:

This work has been supported by the French Atomic Energy commissioning (CEA) in the framework of the MACNA project.

References

[1] Y. de Carlan, J.-L. Bechade, P. Dubuisson, J.-L. Seran, Journal of Nuclear Materials **386-388** (2009) 430-432.
[2] C. Fazio, A. Alamo, A. Almazouzi, S. De Grandis, D. Gomez-Briceno, J. Henry, L. Malerba, M. Rieth, Journal of Nuclear Materials **392** (2009) 316-323.
[3] S. Ukai, T. Narita, A. Alamo, P. Parmentier, Journal of Nuclear Materials **329-333**, Part A (2004) 356-361.
[4] L. Toualbi, C. Cayron, P. Olier, J. Malaplate, M. Praud, M. H. Mathon, D. Bossu, Journal of Nuclear Materials **428**. (2012) 47-53.
[5] A. Nerino, M. Deaver, C. Nagele, J. Reinhart, The Tube and Pipe Journal. (2011) 20-24.
[6] E. Vanegas Marquez, (PhD) Thése de doctorat. ENSMP Mines ParisTech (13/12/2011) (2011) 1-226.
[7] E. Vanegas-Marquez, K. Mocellin, L. Toualbi, Y. de Carlan, R. E. Logé, Journal of Nuclear Materials **420** (2012) 479-490.